

# Investigation of bidirectional converter utilizing battery energy storage for an isolated load system

Karthikeyan Nagarajan<sup>1</sup>, G. D. Anbarasi Jebaselvi<sup>2</sup>

<sup>1</sup>Department of Electrical and Electronics Engineering, Panimalar Engineering College, Chennai, India

<sup>2</sup>Department of Electronics and Communication Engineering, Sathyabama Institute of Science and Technology, Chennai, India

## Article Info

### Article history:

Received Feb 20, 2022

Revised Jan 7, 2023

Accepted Jan 19, 2023

### Keywords:

Asynchronous generator  
Battery energy storage system  
Bidirectional converters  
Hybrid power  
Photovoltaic  
PI controller

## ABSTRACT

To explore the design of a bidirectional isolated converter for usage with battery energy storage systems, the study aims to analyse this investigation. The change resulted in a reduced workload, which is an obvious advantage. We instead think that there will be no effect on the load-carrying capacity due to the increase in production. This research provides an alternating-direct-current renewable energy supply system. Solar, wind, power storage, and a load are included. This is an in-depth discussion of a power conversion converter's control system. Using an energy storage device in addition to the controller is feasible (ESSs). This research resulted in adaptive PI control, which is known for lowering link voltage and faster responses. Using this control system, you can cut down on both transient and static issues and also have a better shot at minimizing defects. MATLAB/Simulink is an application which does simulations. To evaluate the efficacy of an envisioned system, one simulates the systems and compares the results. The results show that the hybrid power supply model proposed may have a substantial effect on the energy supply to the isolated load and can be utilized to build a unique plan for a green data center.

This is an open access article under the [CC BY-SA](https://creativecommons.org/licenses/by-sa/4.0/) license.



## Corresponding Author:

Karthikeyan Nagarajan

Department of Electrical and Electronics Engineering, Panimalar Engineering College  
Chennai, India

Email: karthiee27@gmail.com

## 1. INTRODUCTION

People in today's culture are looking for more energy on a daily basis. In order to make this possible, we will need to produce more energy. It may affect the amount of energy generated from fossil fuels and coal. Renewable energy sources (RES) have a major impact on the world today. Terms like renewable energy sources are used to define resources such as wind and solar. Even though renewable energy sources are efficient, maintaining voltages and frequencies causes problems. To enhance power management, we chose a battery energy storage system (BESS). BESS controls and manages the dispersed generating units' governing and controlling duties [1].

This converter protector is designed to handle a wide range of circuit failure scenarios. In terms of storage, the phrase ESS means energy storage system. In general, it is designed to store energy, and then release it when required. This learning environment is increasingly required in our society for the future generation's growth. Future development will be heavily on how well ESS and RES integrate [2]. The ESS will be in charge of dealing with the converter issues. The most suitable energy storage technology for isolated storage is BESS. Benefit-producing system for power generation has been enhanced because of the installation of isolated BESS. The two-way converter, illustrated in Figure 1, is a simple circuit design that represents an electrical energy storage device [3].

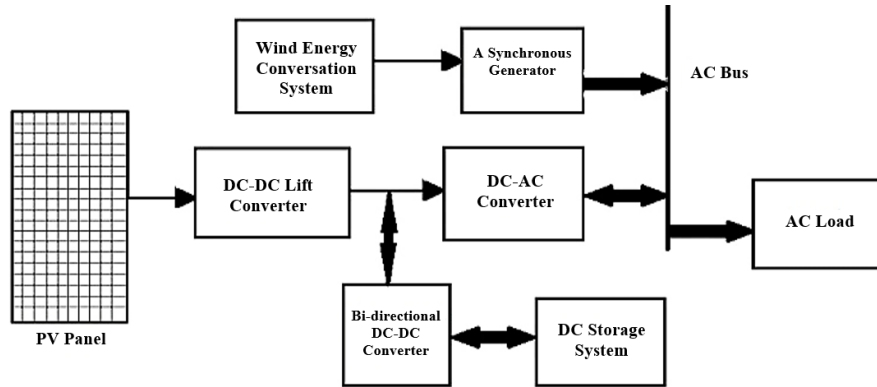


Figure 1. Basic circuit diagram of bidirectional converter for a battery energy storage system

The BESS helps to compensate for distribution system growth, volatility, and unexpected power generation from renewable energy sources. While BESS has not been entirely successful in gaining more technical solutions, such as power quality improvement, energy cost reduction, transmission and distribution network investment modifications, and system service via the use of smart converter technology, it has been successful in resolving power quality issues, reducing energy costs, initiating infrastructure investment, and effecting converter services using smart controller technology. When you connect the battery module in either a serial or parallel manner, you can maintain the capacity of the battery. DC electricity from the BBC is received by converters, which are then responsible for converting the AC power into DC [4].

## 2. PROPOSED CONVERSION SYSTEM

### 2.1. Electrical energy storage system for the proposed conversion system

It is only fair to think about the development of storage facilities that will flatten the day-night curve. The growth of green energy, however, makes other energy solutions more popular. As an example, the increase in renewable power makes storage or backup solutions more important to maintain consistent energy supplies. The system includes measurements like EESS,  $N_{in}$ , and nominal output power (NESS). You should think about your options for power, such as whether you'll have to build your own system to be more powerful. Options include the use of thicker, higher-voltage cables to accommodate a higher demand for power, or a power grid that can support a home that is self-sufficient and doesn't rely on the power company. You will also need to be sure to consider your options for power generation. These include both the maximum depth to which you'll discharge the battery and the efficiency of the energy conversion system, the ability to move a storage medium that has been fully charged from one level to another level, and a system's ability to both store energy and use energy, all of which have various options (p) [5]. Following this, " $E_{tot}$ " is defined as follows.

The Figure 2 represents ESS' contribution to annual electricity usage " $E_{stor}$ " (or " $E_{out}$ "), whereas the power station demand directly fulfilled by the existing power plants is shown by " $E_{dir}$ ". That stat V or other renewable energy sources, is determined by the main operating features of the current power units (which may include PVs or other renewable energy sources).  $e_{ment}$  is common knowledge, therefore I will only mention that 0 to 1 is the range of possible values for "". The true contribution range, which may include PV or other renewable energy sources, is determined by the main operating features of the current power units (which may include PVs or other renewable energy sources) [6].

$$\mathcal{E} = \frac{E_{stor}}{E_{tot}} = 1 - \frac{E_{dir}}{E_{tot}} \quad (1)$$

Table 1 shows the original values for DODL, ESS, and p, as well as an estimate of how long each ESS has been in service (NESS). Sandia National Laboratories has real-world applications. Real-world figures will undoubtedly alter as technology develops and matures, among other factors [7]. These dimensions, the PV the values, characteristics, and elements of ESS are listed: applying the fact that PV generation is only available during the day; the island's total demand may be divided into two categories: this equation can be found in this article (1) [8]. To simplify, the " $E_{t1}$ " and " $E_{t2}$ " symbols may be used to represent the day's energy consumption, while the " $N_{p1}$ " and " $N_{p2}$ " symbols can be used to represent the night's peak network load demand [9]. The relationships of (1) also apply (3).

$$E_{tot} = E_{t1} + E_{t2} \quad (2)$$

$$N_{p-con} = \max \{N_{p1}; N_{p2}\} \quad (3)$$

The results of the research indicate that when the electrical network's peak load demand occurred, " $N_{p-con}$ " indicated this peak load demand [10].

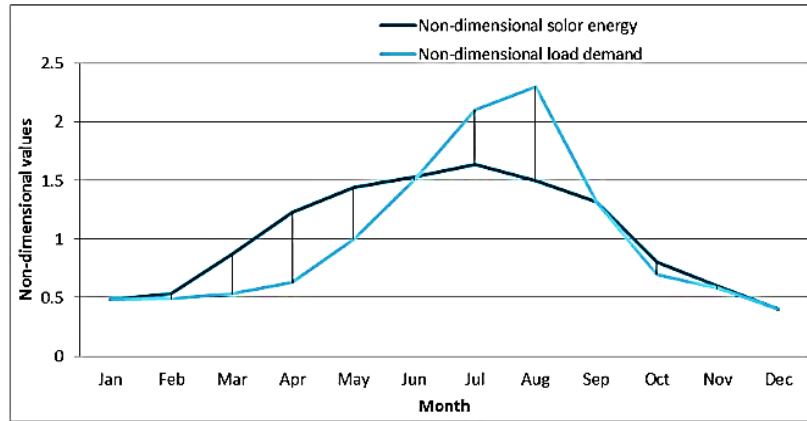


Figure 2. A chart demonstrates how much solar energy contributes to yearly power demand

Table 1. Main characteristics of several storage systems

Different storage	Life period	DODL	Power efficiency	Energy efficiency
Flywheel	16-20	75-80	90-95	80-86
Flow batteries	10-15	100	76-85	61-75
PB-H <sub>2</sub> SO <sub>4</sub>	6-8.1	60.3-70.2	86	76-80.32
Sodium-sulfur	10-15	60.3-80.1	84.3-90.21	76-84.96
CAES	20-40	55-70	80-85	70-80
PHS	30-40	95	78-85	65-80

We may think about the fact that until the ESS fulfills the " $E_{t2}$ " evening demand in total, and that the ESS will only be able to supply additional PV output if the peak load is lower than PV output (parameter " $\xi$ "). (During the rainy season, this results in increased energy use.) A "min EPV" (which refers to the solar photovoltaic (PV) electricity covering a big chunk of  $E_{dir}$ , as defined by (1)) means that the solar power can support both the ER and power delivery to the ESS (total energy efficiency ESS) [11].

$$E_{pv\ min} = (E_{dir} - \delta E) + \frac{E_{stor}}{\eta_{ESS}} = (1 - \varepsilon) * E_{tot} - \delta E + \frac{\varepsilon * E_{tot}}{\eta_{ESS}} \quad (4)$$

The EPV energy yield may be estimated by using the (5). Here  $365 * 24 = 8760$  hrs.

$$E_{pv} = CF_{pv} * 8760 * N_{pv} \quad (5)$$

The capacity factor (which varies between 15% and 25%) of the solar photovoltaic system is " $CF_{pv}$ ." Although the solar irradiation fluctuates throughout the year, A solar photovoltaic generator that cannot produce the projected NPV is simply a power controller that will amplify the current until it reaches a constant current density proportionate to NPV.

Due to this, (1) is used to determine the local electrical network's capacity factor, which is often referred to as  $C_{Fcon}$  (6) [12].

$$CF_{grid} = \frac{E_{tot}}{8760 * N_{p-con}} \quad (6)$$

For the proposed PV-based power plant, the nominal power required is:

$$N_{pv} = \max \left\{ (1 + SF) * N_{p1}; \frac{E_{pv}}{8760 * CF_{pv}} \right\}$$

this can be rewrite as:

$$N_{pv} = N_{p-con} * \max \left\{ (1 + SF) * \frac{N_{p1}}{N_{p-con}}; \frac{CF_P}{CF_{PV}} * \left[ (1 - \varepsilon) - \frac{\delta E}{E_{tot}} + \frac{\varepsilon}{\eta_{ESS}} \right] \right\} \quad (7)$$

In this situation, the Solar photovoltaic power system faces its biggest problem in meeting the demand spike throughout the day, and SF Zero helps guarantee that this occurs, "N<sub>p-con</sub>" is the name given to the load on the local power circuit [13]. To provide an example, "peak power %" on the local network is denoted by the symbol "ξ". The input system's nominal power N<sub>in</sub> may be reduced to the present power surplus. Sometimes, solar-powered generators and explanatory factors are used. Additional costs, along with the period needed to update the system. Our findings suggest: taking into consideration the limited renewable radiation available in the real world, a typical charge and discharge cycle for an ESS may look something like this [14].

$$N_{in} = \lambda * N_{ESS} \leq N_{PV} \quad (8)$$

Where "λ" The length of time it takes to convert available energy into electrical energy is directly proportional to the ratio of charge to discharge periods, and also to the efficacy of the energy transformation mechanisms that are used. This variable may be assumed to have a value anywhere between 1.5 and 3.0 when used in photovoltaic (PV) applications [15].

## 2.2. Circuit diagram for the whole electrical installation of the proposed converter

Whether or not systems have a battery charging mechanism, this is true. Any system would be incomplete without a DC/DC converter [16]. Figure 3 shows a switching-mode regulator converting unconstrained DC input power to regulated DC output voltage using PWM. MOSFETs or IGBTs are utilized as switching devices [17].

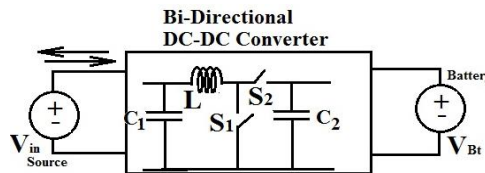


Figure 3. Block diagram of suggested conversion circuit uses a DC-DC converter

In a MOSFET circuit, the drain current increases when the switch is turned on. This means that the diode will not conduct, and therefore, the circuit will not conduct. The voltage between the inductor and the ground is known as when the circuit is in the ON state [18].

$$VL = \frac{D}{1-D} V_{in} \quad (9)$$

In order for the diode to conduct, the MOSFET must be turned off [19]. The voltage across the inductor while the inductor is off is as follows:

$$VL = V_{out} \quad (10)$$

for the reference current to be zero, the net impact of the current must be zero. In order to maintain steady-state operation. Here's what we figure out when we use voltage-second balance [20]:

$$V_{in}D + V_{out}(1-D) = 0 \quad (11)$$

the switching frequency of the conversion is approximately known to be  $D = \text{converter load in ma} / \text{divided by the converter time constant}$ . The formula is:

$$D = \frac{T_{on}}{T_s} \quad (12)$$

the amount of time it takes the transistor to switch, known as the switching time period, occurs during the MOSFET state. The following values are offered as illustrations:

$$V_{out} = -\frac{D}{1-D} V_{in} \quad (13)$$

we were able to construct and simulate a buck boost converter thanks to the help of MATLAB/Simulink [19].

### 3. THE PROPOSED CONVERTER'S CIRCUIT

The suggested converters fall into two distinct categories: DC-DC converters and, more importantly, DC-AC PWM sinusoidal inverters, both of which are used to provide sinusoidal output to the load with minimal distortion.

#### 3.1. DC-AC converter of the proposed converter's circuit

The three-phase DC-AC converters found in electric vehicles, UPS, and renewable energy sources that are tied to the converter are advantageous in the majority of systems [21]. When using a storage battery, two-stage DC-AC converters are utilized to account for changes in voltage [22]. This device features a bidirectional DC-DC converter and a three-phase inverter, as depicted. This DC-DC step of a two-stage DC-AC converter maintains the DC-bus voltage independent of the battery voltage. Effective power management requires just one step [23]. A thorough knowledge of vector analysis and matrix multiplication is required to appreciate three-phase PWM VSI functionality (amplitude modulation ratio- $m_a$ ). To reiterate, this section is focused on the DC/AC converter design [24].

$$V_{Control} = \hat{V}_{Control} \sin(\omega t) \quad (14)$$

Since:

$$V_{AO} = \frac{V_{Control}}{\hat{V}_{tri}} \frac{V_d}{2} = \frac{\hat{V}_{Control}}{\hat{V}_{tri}} \sin(\omega t) \frac{V_d}{2} = m_a \frac{V_d}{2} \sin(\omega t) \quad (15)$$

for  $m_a$  calculation:

$$V_{R-rms} = m_a \frac{V_d}{2\sqrt{2}} \cos\phi \quad (16)$$

$$V_{AB-rms} = \sqrt{3} V_{R-rms} = m_a \frac{\sqrt{3} V_d}{2\sqrt{2}} \cos\phi \quad (17)$$

hence:

$$m_a = \sqrt{3} V_{R-rms} = \frac{V_{AB-rms}}{V_d} \frac{2\sqrt{2}}{\sqrt{3} \cos\phi} \approx 0.936 \quad (18)$$

we can choose  $m_a = 0.936$ ,  $TDH \leq 73\%$ .

PWM produces constant-amplitude, variable-duty-cycle pulses. Modulation is created using a single carrier and reference signal. Comparator outputs a signal after comparing two inputs. Algorithmically produced. The customer expects a reference-wave-like output. Saw tooth and triangle waveforms have a higher carrier frequency than the reference. Through the elimination of higher-order harmonics, a series inductor may be used to improve the efficiency of the load current circuit. We need to stay away from harmonics that aren't in our target area since the harmonics there are lower [25]. A simulation of the proposed converter is shown in Figure 4, replete with blocks representing the different converter parts. The simulated findings are also shown in this simulation circuit diagram (see Figure 4).

#### 3.2. Simulation study of proposed converter

An optimized converter controller, a simulated solar PV system with controllable solar irradiance, an isolated load system with the final output, and a simulated wind energy converter are used to model the proposed converter. MATLAB/Simulink is used for the creation of the simulation blocks. Elements' parameters come straight from the destined analyses.

### 3.3. Controller of the proposed converter's circuit

PI controller raise (also called an impelling sign) next to other controllers with similar tasks, the primary controllers are known as "basic controllers" [26]. Below is a high-level description of the controller's attributes and benefits. The yield illustrates how crucial the data signal is in relation to all other signals in the system [27]. The integrator must be included into the system to determine what system evolves. This manufacturing process reduces SSE, and therefore improves the system's precision. While the advantages of this P-just controller include being able to discard balance, the disadvantages include being less precise. Some things may be true of a set, but not a subset of that set. MATLAB simulation circuit of proposed system is shown in Figure 4.

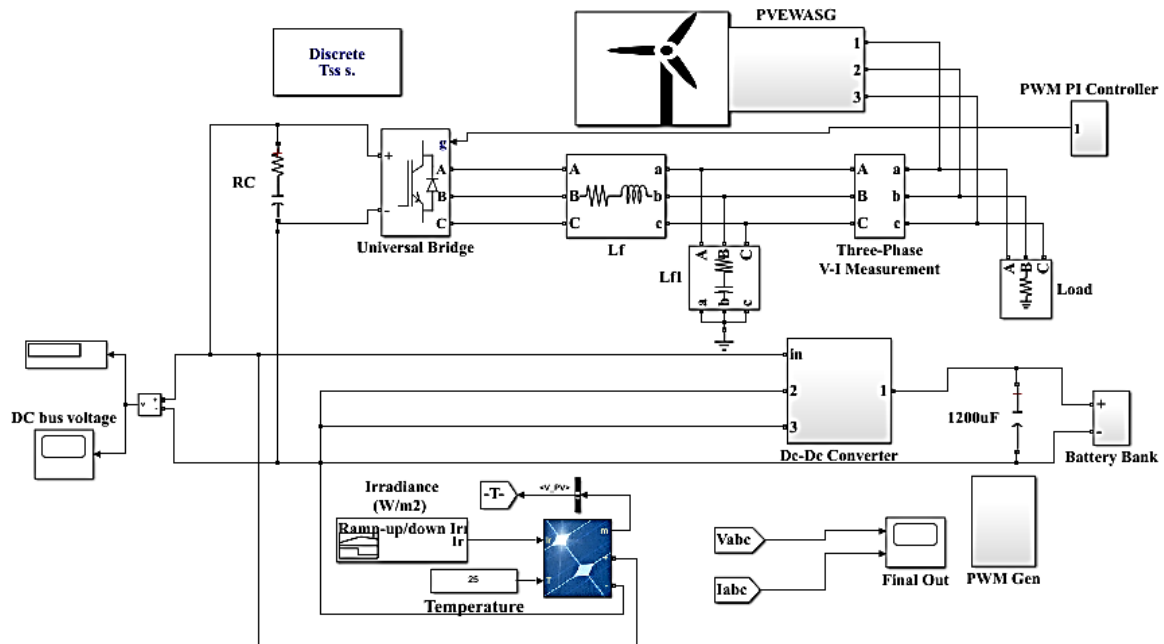


Figure 4. MATLAB/Simulink, simulation diagram of the proposed converter

### 3.4. Solar photovoltaic unit for the proposed systems

Figure 5 depicts the results of varying the solar panel's irradiance input. A chopper or rectifier is used to energize the load, depending on whether the load is connected to the converter or runs on stand-alone power. To take the aforementioned example, you could make use of a battery bank. To manage the voltage supplied across the power switches (MOSFETs, IGBTs), the PWM controller applies PWM modulation to the power supply [28]. A decrease in light reaching the DC side grid as shown in Figure 6 does not prevent the bidirectional converter from drawing power from the battery backup. The goal is to maintain a stable voltage at the output by doing this.

### 3.5. Wind energy conversion unit

Generator rotor speed, as well as load, changes the amplitude and frequency of voltage and frequency, which makes it more difficult to keep voltage levels constant. In terms of the speed of the main mover and the present condition of the load, the frequency of voltage generated in the SEIG is varied. Even if the load on an isolated SEIG is higher, the amplitude of the voltage and frequency are the same, thus there is no change in load. "Because the magnetic field is rotating at a slower pace, this is happening. As the main mover slows down, the voltage and frequency are likely to drop rather than grow [29]. Table 2 provides the modeling parameters for a wind energy conversion system, while Table 3 lists the parameters for DC-DC and DC-AC converters. This study aims to find the ideal conditions for an excitable induction generator (SEIG). Conference presentations were successfully completed and demonstrated a working power system simulation using the Simulink power system block set [30].

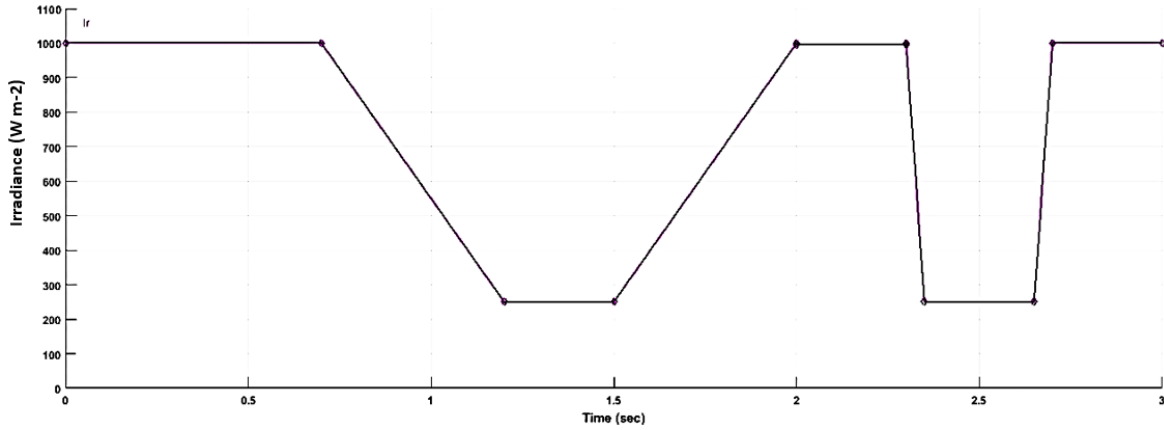


Figure 5. Simulink irradiance input for the proposed circuit with various level

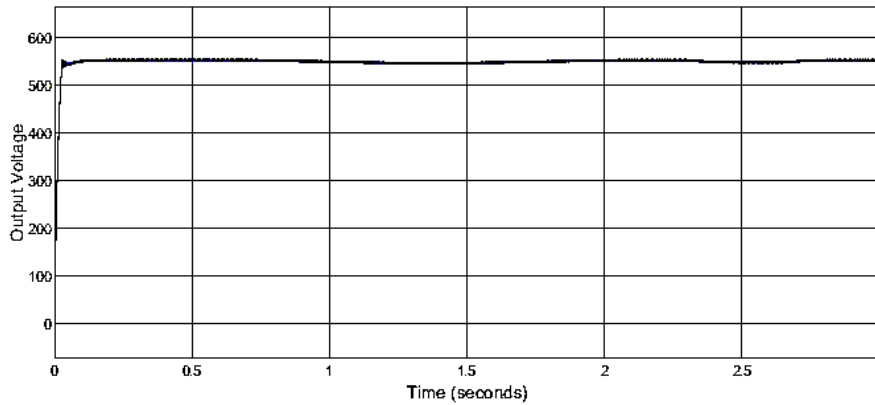


Figure 6. Simulink battery charging and discharging graph of proposed system

Table 2. Parameter of wind energy conversion systems

Asynchronous generator	Wind turbine
Power 5.4 HP	Wind speed at the base 12
Terminal voltage 400 V	Maximum wind speed at base power.73 (pu)
Frequency 50 Hz	Rotational velocity 1.2
Speed 1430 R.P.M	

Table 3. Simulation parameter of DC-DC and DC-AC converter for proposed converter

Basics (DC-DC)	Values	Basics (DC-AC)	Values
Max solar power obtained (Pmax) (W)	365	System inductance (mH) Lf	$(0.1 \times v^2) / (2 \times \pi \times f \times p)$
System inductance La Lb (mH)	0.56	System capacitance (μF)	$(0.05 \times p) / (2 \times \pi \times f \times v^2)$
System capacitance Ca Cb (μF)	148	System resistance Ω	Lf × 100
Output side inductance Lo (mH)	0.98	Output side inductance (mH)	Lf
Output side capacitance Co(μF)	169	Output side capacitance (μF)	Cf
Switching frequency	10 kHz	Load (w) P	6 Kw

#### 4. RESULT AND DISCUSSION

The energy produced by the hybrid system will be the sole kind of electricity delivered to the grid if the load on the isolated system is reduced but the demand for power in the grid system remains high. This is shown in Figure 7 for the digital circuit used in the MATLAB simulation. The only way to achieve this objective is to reduce the load on the regional computer network. It is possible to create 56 distinct solar power configurations by connecting 28 solar panels in series and 2 in parallel. When depleted, each of these solar panels may provide a voltage of around 1013 volts. The voltage may be changed to suit the needs of the load that is plugged in. With an input power of 1000 W/m<sup>2</sup>, the panel may generate the voltage that was



previously described. To get this effect, we used artificial light to look like natural light. This let us control the image's overall brightness and make it look more real.

The wind turbine may travel at a velocity of 12 or 25 meters per second. To maintain a constant velocity of 0.72 psi, we are using a rotating velocimeter. The voltage here is specifically 415 volts. The three-phase induction motor runs at 1435 rpm and 50 hertz, producing 6.4 HP. It runs at a frequency of 50 Hz and has a terminal voltage of 415 volts. The machine generates electricity from the source's asynchronous current and then uses the sinusoidal voltage that acts as an input to the PWM inverter to deliver that electricity to the isolated load. The transmission of power between the load grid and the grid averages 4.5 kW when the voltage between the two is constant at 415 volts. Based on the results of this study, we decided to run two separate simulations. The first simulation results, shown in Figure 7, show no evidence of a bidirectional converter being used. When solar cells produce less than 415 volts of output voltage, they are considered unstable. Regardless, the system retains its steadiness even at very high output voltages. At 0.78 s, the reduction in irradiance commences and continues for the next 1.3 s. After 2.7 s have passed and the system has been reset to its original condition, it will remain in that mode permanently. Once that happens, it rapidly dims back down to its baseline brightness. The second layout incorporates a bidirectional converter and a backup battery without sacrificing the design's original variable irradiance. As a result of this upgrade, the system can withstand a continuous voltage of 415 volts without fluctuating. The data, shown in Figure 8, shows that maintaining a voltage of 415 V over the whole system resulted in a current of 21.3 A across the entire load. The simulation could be completed in three seconds, which would allow for assessing the system's stability at six different irradiance levels. Since it operates in both directions simultaneously, the system may be fully relied upon either way. By using this approach, we are able to fix a problem that has plagued previous attempts to build hybrid systems. Initial conditions will see zero voltage. After receiving a voltage greater than 1013 volts, the device's DC converter will begin accumulating the extra power it generates. By applying 575 volts to the PWM inverter, a sine wave may be produced. The PWM inverter requires 0.04 s, or four times as long as the first 0.02 s, to attain a stable condition during cycle two. About 50 percent of the time, the system will perform as expected.

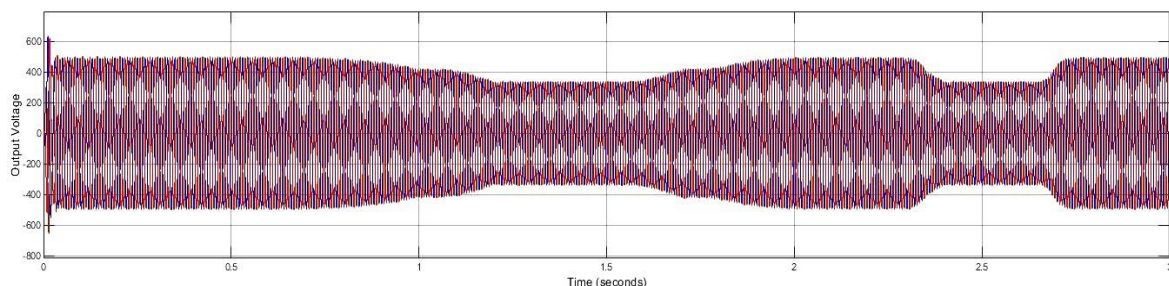


Figure 7. Output voltage of the isolated load side without backup battery system

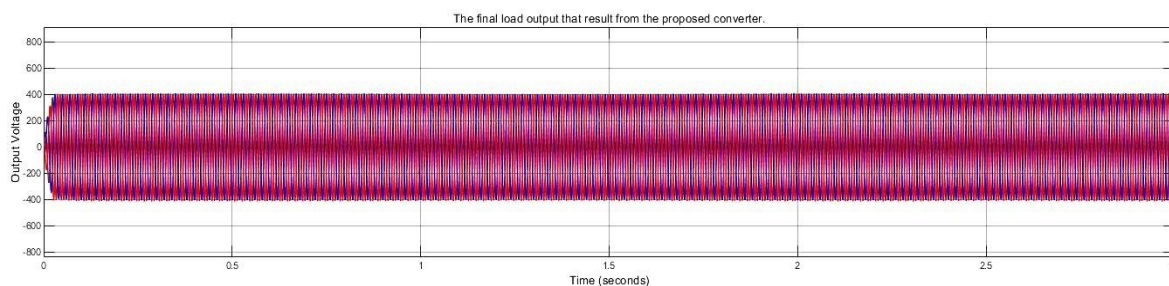


Figure 8. Output voltage of the grid side with backup battery system

## 5. CONCLUSION

In this test, a bidirectional converter connected to a PV panel and backup battery system maintained a DC voltage of 575 volts and supplied 2.1 amps to charge the backup battery. Because of this, even if the PV side of the system was not functioning well, the system was still able to function. Keeping the voltage at



575 volts require the converter to take 6.3 amps from the battery when the irradiance is low, as in the case of 400 w/m<sup>2</sup>. The waveforms of the output voltage and current after the PWM inverter detected the voltage and formed the sinusoidal PWM output of 415 volts to the load after the PWM inverter had previously detected the voltage. Using the PWM sinusoidal inverter, the asynchronous generator was able to achieve its goal of spreading the 9.3 A load current in the form of a sinusoidal waveform. This research allowed us to confirm our suspicions that the bidirectional converter performs as designed and that the system has been stable throughout its deployment and operation. Artificial intelligence-based predictions suggest that response times will get faster in the future because controllers will be smarter.




## REFERENCE

- [1] M. H. Bamzadeh, H. Meyar-Naimi, and M. H. Moradi, "A review of the impact factors on renewable energy policy-making framework based on sustainable development," *Int. J. Renew. Energy Res.*, vol. 11, no. 1, pp. 473–485, 2021, doi: 10.20508/ijrer.v11i1.11768.g8162.
- [2] M. Gunasekaran, V. Krishnasamy, S. Selvam, D. J. Almakhlles, and N. Anglani, "An adaptive resistance perturbation based MPPT algorithm for photovoltaic applications," *IEEE Access*, vol. 8, pp. 196890–196901, 2020, doi: 10.1109/ACCESS.2020.3034283.
- [3] W. S. W. Abdullah, M. Osman, M. Z. A. Ab Kadir, and R. Verayah, "Battery energy storage system (BESS) design for peak demand reduction, energy arbitrage and grid ancillary services," *Int. J. Power Electron. Drive Syst. (IJPEDS)*, vol. 11, no. 1, 2020. doi: 10.11591/ijpeds.v11.i1.pp398-408.
- [4] M. Kharrich *et al.*, "Optimal design of an isolated hybrid microgrid for enhanced deployment of renewable energy sources in Saudi Arabia," *Sustainability*, vol. 13, no. 9, p. 4708, 2021, doi: 10.3390/su13094708.
- [5] F. E. Tahiri, K. Chikh, and M. Khafallah, "Optimal management energy system and control strategies for isolated hybrid solar-wind-battery-diesel power system," *Emerg. Sci. J.*, vol. 5, no. 2, pp. 111–124, 2021, doi: 10.28991/esj-2021-01262.
- [6] R. Ghaffarpour, "Optimal sizing, scheduling and building structure strategies for a risk-averse isolated hybrid energy system in Kish Island," *Energy Build.*, vol. 219, p. 110008, 2020, doi: 10.1016/j.enbuild.2020.110008.
- [7] Y. E. García-Vera, R. Dufo-López, and J. L. Bernal-Agustín, "Optimization of isolated hybrid microgrids with renewable energy based on different battery models and technologies," *Energies*, vol. 13, no. 3, p. 581, 2020, doi: 10.3390/en13030581.
- [8] B. V Rajanna, "Grid connected solar PV system with MPPT and battery energy storage system," *Int. Trans. Electr. Eng. Comput. Sci.*, vol. 1, no. 1, pp. 8–25, 2020.
- [9] T. Chen *et al.*, "Applications of lithium-ion batteries in grid-scale energy storage systems," *Trans. Tianjin Univ.*, vol. 26, no. 3, pp. 208–217, 2020, doi: 10.1007/s12209-020-00236-w.
- [10] H. C. Gils *et al.*, "Modeling flexibility in energy systems-a scenario-based comparison of power sector models," *Renew. Sustain. Energy Rev.*, vol. 158, 2022, doi: 10.1016/j.rser.2021.111995.
- [11] I. Alhamrouni, M. R. Bin Hamzah, M. Salem, A. Jusoh, A. Bin Khairuddin, and T. Sutikno, "A bidirectional resonant converter based on wide input range and high efficiency for photovoltaic application," *Int. J. Power Electron. Drive Syst. (IJPEDS)*, vol. 10, no. 3, p. 1469, 2019, doi: 10.11591/ijpeds.v10.i3.pp1469-1475.
- [12] N. Priyadarshi, S. Padmanaban, M. S. Bhaskar, F. Blaabjerg, and J. B. Holm-Nielsen, "An improved hybrid PV-wind power system with MPPT for water pumping applications," *Int. Trans. Electr. Energy Syst.*, vol. 30, no. 2, p. e12210, 2020, doi: 10.1002/2050-7038.12210.
- [13] H. A. Attia, and F. delAma Gonzalo, "Stand-alone PV system with MPPT function based on fuzzy logic control for remote building applications," *Int. J. Power Electron. Drive Syst. (IJPEDS)*, vol. 10, no. 2, p. 8694, 2019, doi: 10.11591/ijpeds.v10.i2.pp842-851.
- [14] P. C. D. Goud, and R. Gupta, "Solar PV based nanogrid integrated with battery energy storage to supply hybrid residential loads using single-stage hybrid converter," *IET Energy Syst. Integr.*, vol. 2, no. 2, pp. 161–169, 2020, doi: 10.1049/iet-esi.2019.0030.
- [15] Q. Xu, N. Vafamand, L. Chen, T. Dragičević, L. Xie, and F. Blaabjerg, "Review on advanced control technologies for bidirectional DC/DC converters in DC microgrids," *IEEE J. Emerg. Sel. Top. Power Electron.*, vol. 9, no. 2, pp. 1205–1221, 2020, doi: 10.1109/JESTPE.2020.2978064.
- [16] B. Sahoo, S. K. Routray, and P. K. Rout, "A novel sensorless current shaping control approach for SVPWM inverter with voltage disturbance rejection in a dc grid-based wind power generation system," *Wind Energy*, vol. 23, no. 4, pp. 986–1005, 2020, doi: 10.1002/we.2468.
- [17] A. Chatterjee, and D. Chatterjee, "An improved current balancing technique of two-winding IG suitable for wind-PV-based grid-isolated hybrid generation system," *IEEE Syst. J.*, vol. 14, no. 4, pp. 4874–4882, 2020, doi: 10.1109/JSYST.2019.2960151.
- [18] M. W. Abitha, C. Bhuvaneswari, S. M. Shyni, G. M. Sheeba, S. M. Modi, and V. Jaishree, "DC-DC converter based power management for go green applications," *Int. J. Power Electron. Drive Syst. (IJPEDS)*, vol. 10, no. 4, p. 2046, 2019, doi: 10.11591/ijpeds.v10.i4.pp2046-2054.
- [19] Y. Raj Kafle, M. J. Hossain, and M. Kashif, "Quasi-Z-source-based bidirectional DC-DC converters for renewable energy applications," *Int. Trans. Electr. Energy Syst.*, vol. 31, no. 4, p. e12823, 2021, doi: 10.1002/2050-7038.12823.
- [20] A. Suzdalenko, J. Zakis, P. Suskis, and L. Ribickis, "Bidirectional single-loop current sensorless control applied to NPC multi-level converter considering conduction losses," *Int. J. Power Electron. Drive Syst. (IJPEDS)*, vol. 11, no. 4, p. 1945, 2020, doi: 10.11591/ijpeds.v11.i4.pp1945-1957.
- [21] M. Antivachis, J. A. Anderson, D. Bortis, and J. W. Kolar, "Analysis of a synergetically controlled two-stage three-phase DC/AC buck-boost converter," *CPSS Trans. Power Electron. Appl.*, vol. 5, no. 1, pp. 34–53, 2020, doi: 10.24295/CPSSPEA.2020.00004.
- [22] W. Pinthurat, and B. Hredzak, "Decentralized frequency control of battery energy storage systems distributed in isolated microgrid," *Energies*, vol. 13, no. 11, p. 3026, 2020, doi: 10.3390/en13113026.
- [23] S. Adarsh, and H. Nagendrappa, "Duty ratio control of three port isolated bidirectional asymmetrical triple active bridge DC-DC converter," *Int. J. Power Electron. Drive Syst. (IJPEDS)*, vol. 12, no. 2, p. 943, 2021, doi: 10.11591/ijpeds.v12.i2.pp943-956.
- [24] S. Nagaraj, R. Ranihemamalini, and L. Rajaji, "Design and analysis of controllers for high voltage gain DC-DC converter for PV panel," *Int. J. Power Electron. Drive Syst. (IJPEDS)*, vol. 11, no. 2, p. 594, 2020, doi: 10.11591/ijpeds.v11.i2.pp594-604.




- [25] A. Subramanian, and S. Kr, "Review of multiport isolated bidirectional converter interfacing renewable and energy storage system," *Int. J. Power Electron. Drive Syst.*, vol. 11, no. 1, p. 466, 2020, doi: 10.11591/ijpeds.v11.i1.pp466-467.
- [26] S. W. Shneen, D. H. Shaker, and F. N. Abdullah, "Simulation model of PID for DC-DC converter by using MATLAB," *Int. J. Electr. Comput. Eng. (IJECE)*, vol. 11, no. 5, 2021, doi: 10.11591/ijece.v11i5.pp3791-3797.
- [27] P. B. L. Neto, O. R. Saavedra, and D. Q. Oliveira, "The effect of complementarity between solar, wind and tidal energy in isolated hybrid microgrids," *Renew. Energy*, vol. 147, pp. 339–355, 2020, doi: 10.1016/j.renene.2019.08.134.
- [28] T. Toumi, A. Allali, O. Abdelkhalak, A. Ben Abdelkader, A. Meftouhi, and M. A. Soumeur, "PV integrated single-phase dynamic voltage restorer for sag voltage, voltage fluctuations and harmonics compensation," *Int. J. Power Electron. Drive Syst. (IJPEDS)*, vol. 11, no. 1, p. 547, 2020, doi: 10.11591/ijpeds.v11.i1.pp547-554.
- [29] H. Shayeghi, F. Monfaredi, A. Dejamkhooy, M. Shafie-khah, and J. P. S. Catalão, "Assessing hybrid supercapacitor-battery energy storage for active power management in a wind-diesel system," *International Journal of Electrical Power & Energy Systems*, vol. 125, p. 106391, 2021, doi: 10.1016/j.ijepes.2020.106391.
- [30] M. M. Rana, M. F. Romlie, and M. F. Abdullah, "Peak load shaving in isolated microgrid by using hybrid PV-BESS system," *International Journal of Emerging Trends in Engineering Research*, vol. 8, no. 1.1, pp. 7–14, 2020, doi: 10.30534/ijeter/2020/0281.12020.

## BIOGRAPHIES OF AUTHORS



**Karthikeyan Nagarajan**    received his B.E. from Arasu Engineering College, affiliated with Anna University, in 2008, and his ME from Saranathan College of Engineering which is also affiliated with Anna University, in 2010. Presently, he is working as an Assistant Professor in the Department of EEE at Panimalar Engineering College, Chennai. He is presently pursuing his PhD at Sathyabama Institute of Science and Technology. He has published a few papers in national and international journals and conferences. He has a total teaching experience of 10 years. Electrical Machines, Power Electronics and Drives, and Renewable Energy Systems are among his research interests. He can be contacted at email: karthiee27@gmail.com.



**G. D. Anbarasi Jebaselvi**    has completed her B.E. in Government College of Engineering, Tirunelveli, in 1990 and pursued her M.E. in College of Engineering, Guindy, Anna University and obtained her degree by 2003. She had a strong passion towards teaching profession and her career started as a Lecturer in Sathyabama Engineering College and reached its peaks, been awarded a doctorate degree by the same university. Her research interest includes renewable energy sources particularly wind and solar systems, modeling of wind electric generators, Solar power technologies and power electronic converters. She has published around 25 papers including many Scopus indexed ones and one of the papers appeared in a high rated journal. Her research findings have been explicit through her paper presentations and publications in various international conferences and journals. She can be contacted at email: anbarasi.jebaselvi@gmail.com.